Nanosecond-pulsed, dual-wavelength, passively Q-switched ytterbium-doped bulk laser based on few-layer MoS_2 saturable absorber

Fei Lou,[1] Ruwei Zhao,[1] Jingliang He,[1,*] Zhitai Jia,[1] Xiancui Su,[1] Zhaowei Wang,[1]
Jia Hou,[1] and Baitao Zhang[1,2]

[1]State Key Laboratory of Crystal Materials, Shandong University, Jinan 250100, China
[2]e-mail: bai3697@126.com
*Corresponding author: jlhe@sdu.edu.cn

Received November 14, 2014; revised January 7, 2015; accepted January 21, 2015;
posted January 26, 2015 (Doc. ID 226807); published March 23, 2015

A compact saturable absorber mirror (SAM) based on few-layer molybdenum disulfide (MoS_2) nanoplatelets was fabricated and successfully used as an efficient saturable absorber (SA) for the passively Q-switched solid-state laser at 1 μm wavelength. Pulses as short as 182 ns were obtained from a ytterbium-doped (Yb:LGGG) bulk laser Q-switched by the MoS_2 SAM, which we believe to be the shortest one ever achieved from the MoS_2 SAs-based Q-switched bulk lasers. A maximum average output power of 0.6 W was obtained with a slope efficiency of 24%, corresponding to single pulse energy up to 1.8 μJ. In addition, the simultaneous dual-wavelength Q-switching at 1025.2 and 1028.1 nm has been successfully achieved. The results indicate the promising potential of few-layer MoS_2 nanoplatelets as nonlinear optical switches for achieving efficient pulsed bulk lasers.

OCIS codes: (140.3580) Lasers, solid-state; (160.4330) Nonlinear optical materials; (160.4236) Nanomaterials.
http://dx.doi.org/10.1364/PRJ.3.000A25

1. INTRODUCTION

For the generation of nanosecond pulses and subnanosecond pulses, passive Q-switching (QS) and mode locking by incorporation of saturable absorbers (SAs) have been extensively employed as a consequence of their excellent mechanical stability and compactness. The SA plays a key role in periodically modulating the intracavity loss and turning the continuous-wave (CW) laser into pulse trains. Cr^{4+}:YAG as a powerful SA has been widely used in solid-state lasers, while it has some limitations such as the relatively high cost. The application of semiconductor saturable absorber mirrors (SESAMs) as Q-switchers is limited because of their complicated and expensive manufacturing technology and narrow operation waveband. Thanks to the excellent saturable absorption properties and high thermal stability, low-dimensional carbon nanostructures have emerged as promising SAs in recent years [1–4]. With graphene-based SAs, ultrafast pulse generation in the wavelength range between 0.8 and 2.5 μm has been realized [5–11]. As for the graphene-based QS operation, systematic studies in the spectral region of 0.9 to 2 μm are also performed with impressive results given out [12–16]. The success of graphene being applied in pulsed lasers motivates the exploration of other graphene-like two-dimensional (2D) materials. Recently, a rising Dirac material called topological insulators (TIs) with an insulating bulk state and gapless Dirac-type surface/edge has attracted great interest in condensed-matter physics, which has been verified with broadband saturable absorption properties experimentally [17–19]. Utilizing the saturable absorption of TI, Tang *et al.* obtained pulses with pulse widths of 6.3 μs from an Er:YAG bulk laser by using a Bi_2Te_3 SA [20]. Using a Bi_2Se_3 SA and a Nd:YVO_4 crystal, Q-switched pulse widths as short as 250 ns are achieved, which are the shortest ones from the TI-based Q-switched lasers [21]. In the fiber lasers, TI-based SA devices also demonstrate promising characteristics for realizing pulsed lasers [22–25].

In addition, molybdenum disulfide (MoS_2) as a typical transition-metal dichalcogenide is now under continuously rising attention due to its thickness-dependent electronic and optical properties. Unlike graphene, which possesses very weak second-order nonlinearity, few-layer MoS_2 shows an interesting layer-dependent [26,27] or orientation-dependent second-order nonlinearity [28], determined by the unique symmetry of its lattice structure. The MoS_2 dispersions have shown stronger saturable absorption responses than graphene dispersions [29]. Furthermore, it was interesting to note, by introducing suitable defects in MoS_2, the bandgap of MoS_2 atomic layers decrease to 0.26 eV, corresponding to an absorption edge up to about 4.7 μm [30]. With broadband few-layer MoS_2 as SAs, passively Q-switched and ultrafast lasers have been realized [30–36]. Zhang *et al.* reported a MoS_2-based optical fiber SA device that fits the mode-locking operation of an ytterbium-doped fiber laser and experimentally generates nanosecond dissipative soliton pulses at 1054 nm [32]. At 1.5 μm wavelength region, the ultrashort pulse generation from an erbium-doped fiber laser mode-locked by multilayer MoS_2-based SAs were also demonstrated [33,34]. In bulk lasers employing the MoS_2 samples as SAs, a passively Q-switched Nd:$GdVO_4$ laser at a wavelength of 1.06 μm has been realized [30], from which the minimum pulse duration, maximum output power, and maximum pulse energy of 970 ns, 227 mW, and 0.31 μJ were obtained, respectively. Moreover, the MoS_2 samples were prepared with the pulsed laser deposition technique by employing an expensive and complicated instrument. In addition, Xu *et al.* reported a three-layer MoS_2 Q-switched Nd:YAP laser at 1079.5 nm [35]. A maximum average output power of 0.26 W was obtained with a slope efficiency of 10.6%. The maximum pulse energy and the shortest pulse width were 1.1 μJ and 227 ns, respectively.

Here, a compact MoS_2-based saturable absorber mirror (SAM) was fabricated and successfully employed in realizing a diode-pumped passively Q-switched ytterbium-doped (Yb:LGGG) bulk laser. The generated pulses with the shortest pulse width of 182 ns and the highest single pulse energy of 1.8 μJ hold records among the MoS_2 SA-based Q-switched solid-state lasers that have been reported, to our knowledge. The corresponding slope efficiency of the passively Q-switched laser could reach 24%. In addition, the simultaneous dual-wavelength QS at 1025.2 and 1028.1 nm has been successfully achieved. The results here suggest that few-layer MoS_2 is an efficient Q-switch for achieving short solid-state laser pulses in nanosecond regime.

2. PREPARATION AND CHARACTERIZATION OF MoS_2

Single or multiple layers of MoS_2 flakes were exfoliated from commercially available crystals of molybdenite (SPI Supplied Brand Moly Disulfide) using the scotch-tape micromechanical cleavage technique method pioneered for the production of graphene [37,38]. The MoS_2 sheets were dispersed in an ethanol solution. These MoS_2 sheets can be directly deposited onto varieties of substrates by the spin-coating method. To confirm that the bulk MoS_2 was exfoliated into a few-layer structure, we measured the Raman spectroscopy of our sample, as shown in Fig. 1. The two characteristic peaks E^1_{2g} and A_{1g} of our sample occurred at 382 and 405 cm^{-1}. The red shift of the shear mode (E^1_{2g}) compared with bulk MoS_2 implied a successful exfoliation of the bulk MoS_2 [39].

A piece of quartz was employed as the substrate in this work. The dielectric coatings consisting of dozens of SiO_2/TiO_2 thin layers with a high refractive index contrast were deposited on it. These thin polymer layers were essential to modify the reflectivity of the substrate to 95% at 1025 nm

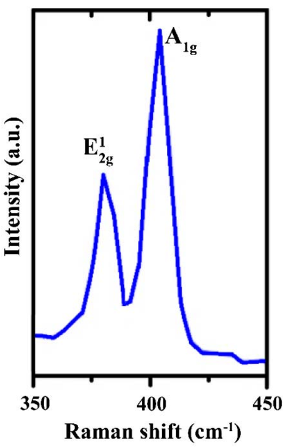

Fig. 1. Raman spectra of the exfoliated MoS_2.

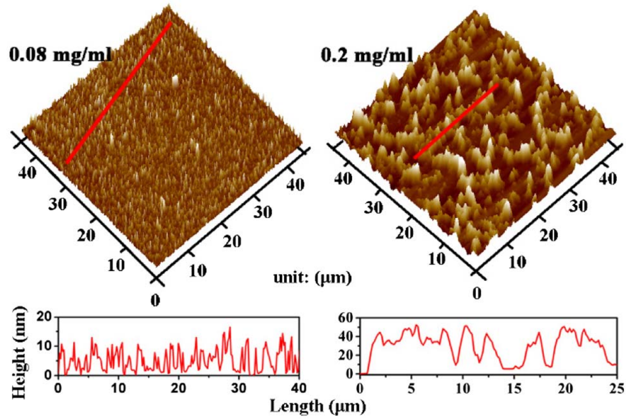

Fig. 2. AFM scan image of the MoS_2 surface and the typical height profiles of MoS_2 thin films.

with a 15 nm band. The MoS_2 solution followed by 30 min sonication was spin coated onto it and then dried in a vacuum oven at 100°C for 24 h. By applying these steps, a compact MoS_2-based SAM was successfully fabricated.

To meet the requirement of stable pulsed solid-state lasers, the area of MoS_2 should cover the oscillating modes. Figure 2 demonstrates the morphology of MoS_2 sheets, which are spin-coated on the mica substrate with two different concentrations of MoS_2 dispersions (0.08 and 0.2 mg/ml) taken by an atomic force microscope (AFM). The surface morphology shows clearly that MoS_2 flakes reunite easily at the high concentration case (0.2 mg/ml). In order to obtain uniform and thinner film, the concentration of MoS_2 dispersion for use in all other tests was diluted to 0.08 mg/ml. In this situation, it is can be seen that the average thickness of the film is about 10 nm. By assuming that the height of a single layer is 0.65 nm [37] and the MoS_2 layers bond via the Van der Waals interaction, the average number of layers in the film is calculated to be ~15. According to the previous results, the indirect bandgap of the 15-layer MoS_2 is ~0.87 eV, which corresponds to an absorption edge up to 1.4 μm [40]. Figure 3(a) shows the scanning electron microscopy (SEM) image of the as-prepared MoS_2 nanosheets. The result indicates that MoS_2 has a good distribution uniformity on the quartz substrate, and it is in good agreement with the AFM images. The balanced twin detector technology was used for the measurement of saturable absorption of the MoS_2 sample on an uncoated quartz [41]. A homemade passively mode-locked $Nd:YVO_4$ laser with the pulse duration of 15 ps and wavelength of 1.06 μm is used as the pump source. Figure 3(b) shows the nonlinear transmission of the MoS_2 sample. The modulation depth of our MoS_2 SA is estimated to be ~9.7% at 1 μm. Considering

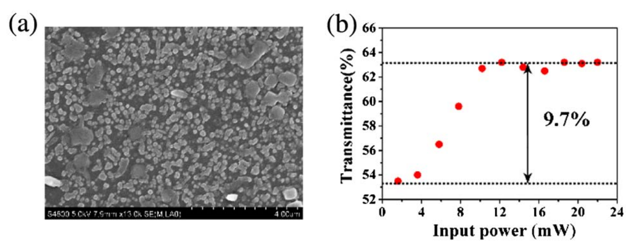

Fig. 3. (a) SEM image of MoS_2 thin film. (b) Relation between transmittance of MoS_2 samples and input power with the wavelength of 1 μm.

the Fresnel reflection loss of about 8% for both sides of the pure quartz, the nonsaturable loss of our SA was calculated to be 28.8%.

3. RESULT AND DISCUSSION

A 25 mm long, standard two-mirror resonator was used to evaluate the performance of the MoS_2 SAM. The uncoated 3 mm long Yb:$(Lu_xGd_{1-x})_3Ga_5O_{12}$ (Yb:LGGG) crystal with a square aperture of 4 mm × 4 mm and 6% Yb concentration was employed as the gain medium. The pump source was a fiber-coupled laser diode at 935 nm, with a 400 μm fiber diameter. The output beam was reimaged into the gain medium with 200 μm radius by an optical collimation system. The crystal was cooled with water at a constant temperature of 13 °C.

Initially, we investigated the performance of the CW Yb:LGGG laser by replacing the MoS_2 SAM with a plane quartz reflector with 5% transmittance around 1025 nm. The average output power was plotted in Fig. 4 as a function of the absorbed pump power. The laser oscillation was realized at the threshold pump power of 0.98 W. 1.8 W output power was obtained under the absorbed pump power of 3.85 W, resulting in a slope efficiency of 63.8%. Noise-like pulses were accidentally observed in this free-running regime, which should account for the intracavity intensity fluctuation and the Kerr-lens effect of the gain medium. It was noted that careful cavity alignment did not help much in stabilizing the pulses.

When the MoS_2 SAM was used to substitute the quartz reflector, as expected, the laser was switched from above free running to QS operation as soon as the absorbed pump power exceeded the threshold of 1.65 W. The relationship between the average output power and absorbed pump power is plotted in Fig. 4. It can be seen that the average output power increased linearly with the incident pump power. No pump saturation was observed even if the incident pump power increased to 3.85 W. Under this absorbed pump power, an average output power of 0.6 W was obtained, corresponding to a slope efficiency of 24%. The pulse width and repetition rate depending on the absorbed pumped power were recorded by a digital oscilloscope and presented in Fig. 5. The pulse width presented a rapid drop from 820 ns to a minimum data of 182 ns in pulse width with the increase of the pump power from the threshold to 3.85 W, while an increase in repetition rate from 94 to 333 kHz occurred.

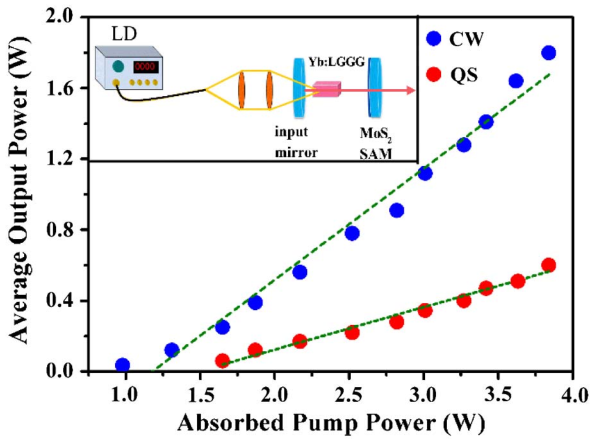

Fig. 4. Average output power versus incident pump power for continuous wave and QS operation. Inset: Configuration of the MoS_2 Q-switched Yb:LGGG laser.

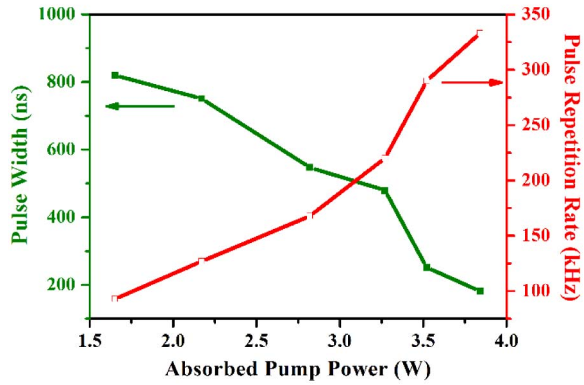

Fig. 5. Pulse width and repetition rate versus absorbed pump power for QS operation.

We believe the 182 ns pulse, as shown in Fig. 6, to be the shortest one ever reported for the passively Q-switched bulk lasers using MoS_2-based SAs. The maximum single pulse energy of 1.8 μJ was achieved under the incident pump power of 3.85 W, which was higher than any previous result [30,35]. The variations of the pulse repetition rates with pump power are shown in Fig. 7. The pulse stability in the experiment seems not perfect. We think the possible reasons are as follows: (1) the inhomogeneity of SA; (2) the simple plane–plane cavity structure, which induced some instability; (3) the thermal accumulation in the SA. Therefore, we believe that the stability could be improved by optimizing the quality of SA and the design of laser cavity.

Figure 8(a) exhibits a typical output dual-wavelength spectrum at a pump power of 3.85 W. To the best of our knowledge, this was the first work realizing a simultaneous dual-wavelength Q-switched laser operation based on the MoS_2 SA. For a homogeneous broadening laser system, it would be difficult to realize multiwavelength operation without any spectral filtering, because the oscillating laser mode will consume the same inversion population. However, the LGGG host crystal belongs to a disordered crystal structure, which makes the doped Yb active ions run in the inhomogeneous broadening regime. In this regime, the Yb ions in different crystal sites would tend to emit different peak wavelengths independently since they consume a different inversion

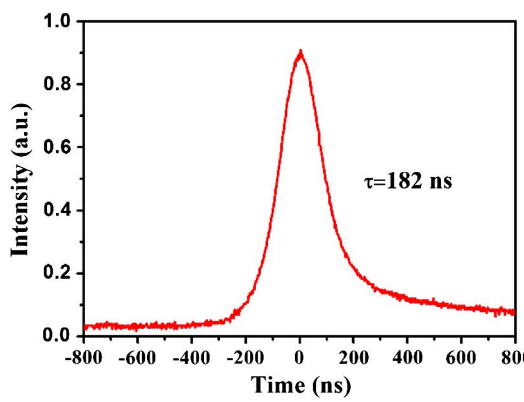

Fig. 6. 182 ns Q-switched pulse profile under the incident pump power of 3.85 W.

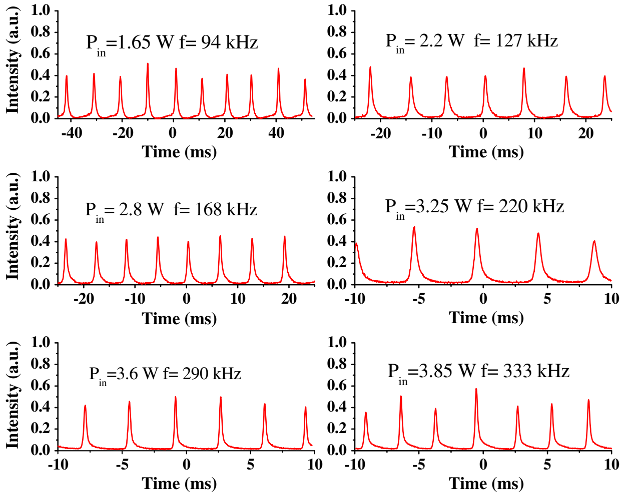

Fig. 7. Pulse trains of MoS_2 Q-switched Yb:LGGG laser under the different incident pump power.

population. When working in the passive QS regime, the introduced nonsaturable loss would influence the emission spectrum especially for the three-level laser system and usually blue shift the emission peak in comparison with the free-running operation. On the other hand, the peak wavelength with low gain would be prevented from oscillating. But if the gain is comparable to compensate the loss, the corresponding laser mode will survive. In summary, we attribute the dual-wavelength operation mainly to the disordered structure of Yb:LGGG crystal. The dual-wavelength operation was also observed in the SESAM mode-locked Yb:LGGG laser in our previous work [42].

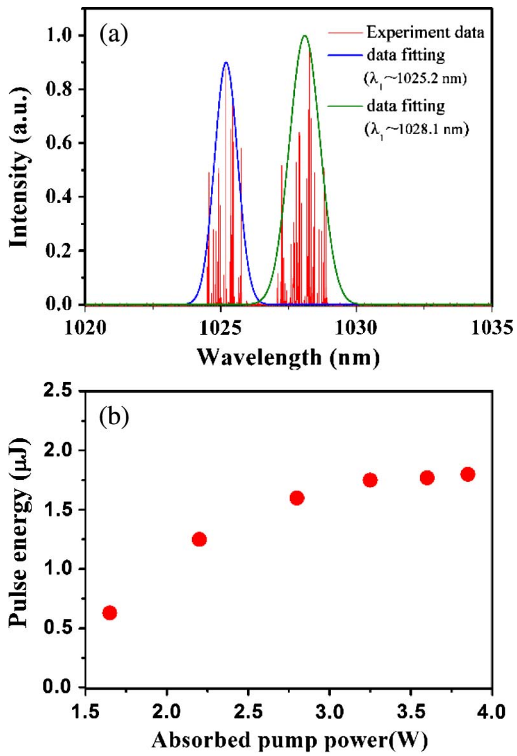

Fig. 8. (a) Typical spectrum of the MoS_2 Q-switched Yb:LGGG laser under the incident pump power of 3.85 W. (b) Pulse energy versus the pump power.

As is shown in Fig. 8(b), the single pulse energy showed a saturation tendency with the absorbed pump power. If we further increased the pump power, obvious deterioration happened to the QS operation. A maximum single pulse energy of 1.8 μJ was obtained, corresponding to an intracavity intensity of 2.8×10^4 W/cm^2 on the MoS_2 sheets. The pulse energy saturation indicated an oversaturation on the MoS_2 SA, which would lead to the deteriorated QS operation. In addition, some studies have addressed the thermal conductivity (κ) of MoS_2. A Raman study has estimated that few-layered MoS_2 has a κ of 52 W/m K in [43]. Using *ab initio* calculations, the thermal conductivity of monolayer MoS_2 with a typical sample size of 1 μm was calculated to be 83 W/m K at room temperature [44]. While for the single-layer graphene, this value is found to be 5000 W/m K. Moreover, the nonsaturable loss of MoS_2-based SAs are in the range of 20%-35% [33,34], which is larger than that of graphene SAs. Using a MoS_2 SA that was fabricated with the MoS_2 solution of 0.2 mg/ml concentration, sparks (damage) could be easily observed on the SAM surface even in a low pump level in the experiment. Basically, the MoS_2 SA has large nonsaturable loss introducing a large impurity absorption in the SA, which will cause the heat accumulation. From this side, the subsequent thermal effect on MoS_2 SA would further deteriorate the lasing performance together with the oversaturation. By employing MoS_2 sheets with larger lateral size and substituting the SAM substrate from quartz to silicon carbide (SiC) ($\kappa = 318$ W/m K), higher output power with larger pulse energy can be expected.

4. CONCLUSIONS

In summary, we have experimentally demonstrated an efficient diode-pumped passively Q-switched bulk laser exploiting a MoS_2 SAM. The laser pulses with the shortest pulse width of 182 ns and the highest single pulse energy of 1.8 μJ among the MoS_2 SA-based solid-state laser were generated. In addition, the simultaneous dual-wavelength QS at 1025.2 and 1028.1 nm has been successfully achieved. The results, to the best of our knowledge, are records among the MoS_2 SA-based solid-state lasers that have been reported and indicate that MoS_2 is a kind of promising SA for generating high efficiency and energy pulses with hundreds kHz repetition rates.

ACKNOWLEDGMENTS

This work was supported by the National Natural Science Foundation of China (Grant Nos. 51321091, 61275142, 61308042, and 91022003) and China Postdoctoral Science Foundation (Grant Nos. 2013M531594, 2014T70633).

REFERENCES

1. T. Hasan, Z. Sun, F. Wang, F. Bonaccorso, P. H. Tan, A. G. Rozhin, and A. C. Ferrari, "Nanotube-polymer composites for ultrafast photonics," Adv. Mater. **21**, 3874–3899 (2009).
2. Q. L. Bao, H. Zhang, Y. Wang, Z. H. Ni, Y. L. Yan, Z. X. Shen, K. P. Loh, and D. Y. Tang, "Atomic layer graphene as saturable absorber for ultrafast pulsed laser," Adv. Funct. Mater. **19**, 3077–3083 (2009).
3. A. Martinez, K. Fuse, and S. Yamashita, "Mechanical exfoliation of graphene for the passive mode-locking of fiber lasers," Appl. Phys. Lett. **99**, 121107 (2011).
4. H. Zhang, Q. L. Bao, D. Y. Tang, L. M. Zhao, and K. P. Loh, "Large energy soliton erbium-doped fiber laser with a

graphene-polymer composite mode locker," Appl. Phys. Lett. **95**, 141103 (2009).
5. I. H. Baek, H. W. Lee, S. Bae, B. H. Hong, Y. H. Ahn, D. Yeom, and F. Rotermund, "Efficient mode-locking of sub-70-fs Ti:sapphire laser by graphene saturable absorber," Appl. Phys. Express **5**, 032701 (2012).
6. F. Lou, L. Cui, Y. B. Li, J. Hou, J. L. He, Z. T. Jia, J. Q. Liu, B. T. Zhang, K. J. Yang, Z. W. Wang, and X. T. Tao, "High-efficiency femtosecond $Yb:Gd_3Al_{0.5}Ga_{4.5}O_{12}$ mode-locked laser based on reduced graphene oxide," Opt. Lett. **38**, 4189–4192 (2013).
7. J. L. Xu, X. L. Li, J. L. He, X. P. Hao, Y. Z. Wu, Y. Yang, and K. J. Yang, "Performance of large-area few-layer graphene saturable absorber in femtosecond bulk laser," Appl. Phys. Lett. **99**, 261107 (2011).
8. E. Ugolotti, A. Schmidt, V. Petrov, J. W. Kim, D. Yeom, F. Rotermund, S. Bae, B. H. Hong, A. Agnesi, C. Fiebig, G. Erbert, X. Mateos, M. Aguiló, F. Diaz, and U. Griebner, "Graphene mode-locked femtosecond Yb:KLuW laser," Appl. Phys. Lett. **101**, 161112 (2012).
9. J. Ma, G. Q. Xie, P. Lv, W. L. Gao, P. Yuan, L. J. Qian, H. H. Yu, H. J. Zhang, J. Y. Wang, and D. Y. Tang, "Graphene mode-locked femtosecond laser at 2 μm wavelength," Opt. Lett. **37**, 2085–2087 (2012).
10. M. N. Cizmeciyan, J. W. Kim, S. Bae, B. H. Hong, F. Rotermund, and A. Sennaroglu, "Graphene mode-locked femtosecond Cr:ZnSe laser at 2500 nm," Opt. Lett. **38**, 341–343 (2013).
11. J. Liu, Y. G. Wang, Z. S. Qu, L. H. Zheng, L. B. Su, and J. Xu, "Graphene oxide absorber for 2 μm passive mode-locking $Tm:YAlO_3$ laser," Laser Phys. Lett. **9**, 15–19 (2012).
12. S. Han, X. Li, H. Xu, Y. Zhao, H. Yu, H. Zhang, Y. Wu, Z. Wang, X. Hao, and X. Xu, "Graphene Q-switched 0.9-μm $Nd:La_{0.11}Y_{0.89}VO_4$ laser," Chin. Opt. Lett. **12**, 011401 (2014).
13. X. L. Li, J. L. Xu, Y. Z. Wu, J. L. He, and X. P. Hao, "Large energy laser pulses with high repetition rate by graphene Q-switched solid-state laser," Opt. Express **19**, 9951–9955 (2011).
14. J. L. Xu, X. L. Li, J. L. He, X. P. Hao, Y. Yang, Y. Z. Wu, S. D. Liu, and B. T. Zhang, "Efficient graphene Q-switching and mode locking of 1.34 μm neodymium lasers," Opt. Lett. **37**, 2652–2654 (2012).
15. Z. X. Zhu, Y. Wang, H. Chen, H. T. Huang, D. Y. Shen, J. Zhang, and D. Y. Tang, "A graphene-based passively Q-switched polycrystalline Er:YAG ceramic laser operation at 1645 nm," Laser Phys. Lett. **10**, 055801 (2013).
16. J. Hou, B. T. Zhang, J. L. He, Z. W. Wang, F. Lou, J. Ning, R. W. Zhao, and X. C. Su, "Passively Q-switched 2 μm Tm:YAP laser based on graphene saturable absorber mirror," Appl. Opt. **53**, 4968–4971 (2014).
17. M. Z. Hasan and C. L. Kane, "Colloquium: topological insulators," Rev. Mod. Phys. **82**, 3045–3067 (2010).
18. X. L. Qi and S. C. Zhang, "Topological insulators and superconductors," Rev. Mod. Phys. **83**, 1057–1110 (2011).
19. H. Yu, H. Zhang, Y. Wang, C. Zhao, B. Wang, S. Wen, H. Zhang, and J. Wang, "Topological insulator as an optical modulator for pulsed solid-state lasers," Laser Photon. Rev. **7**, L77–L83 (2013).
20. P. Tang, X. Zhang, C. Zhao, Y. Wang, H. Zhang, D. Shen, S. Wen, D. Tang, and D. Fan, "Topological insulator Bi_2Te_3 saturable for the passive Q-switching operation of an in-band pumped 1645-nm Er:YAG ceramic laser," IEEE Photon. J. **5**, 1500707 (2013).
21. F. Q. Jia, H. Chen, P. Liu, Y. Z. Huang, and Z. Q. Luo, "Nanosecond-pulsed, dual-wavelength passively Q-switched c-cut $Nd:YVO_4$ laser using a few-layer Bi_2Se_3 saturable absorber," IEEE J. Sel. Top. Quantum Electron. **21**, 1601806 (2015).
22. C. Zhao, Y. Zou, Y. Chen, Z. Wang, S. Lu, H. Zhang, S. Wen, and D. Tang, "Wavelength-tunable picosecond soliton fiber laser with topological insulator: Bi_2Se_3 as a mode locker," Opt. Express **20**, 27888–27895 (2012).
23. Y. Chen, C. Zhao, H. Huang, S. Chen, P. Tang, Z. Wang, S. Lu, H. Zhang, S. Wen, and D. Tang, "Self-assembled topological insulator: Bi_2Se_3 membrane as a passive Q-switcher in an erbium-doped fiber laser," J. Lightwave Technol. **31**, 2857–2863 (2013).
24. C. Zhao, H. Zhang, X. Qi, Y. Chen, Z. Wang, S. Wen, and D. Tang, "Ultra-short pulse generation by a topological insulator based saturable absorber," Appl. Phys. Lett. **101**, 211106 (2012).
25. Z. Q. Luo, Y. Z. Huang, J. Weng, H. H. Cheng, Z. Q. Lin, B. Xu, Z. P. Cai, and H. Y. Xu, "1.06 μm Q-switched ytterbium-doped fiber laser using few-layer topological insulator Bi_2Se_3 as a saturable absorber," Opt. Express **21**, 29516–29522 (2013).
26. Y. L. Li, Y. Rao, K. F. Mak, Y. M. You, S. Y. Wang, C. R. Dean, and T. F. Heinz, "Probing symmetry properties of few-layer MoS_2 and h-BN by optical second-harmonic generation," Nano Lett. **13**, 3329–3333 (2013).
27. R. Wang, H. C. Chien, J. Kumar, N. Kumar, H. Y. Chiu, and H. Zhao, "Third-harmonic generation in ultrathin films of MoS_2," ACS Appl. Mater. Interface **6**, 314–318 (2014).
28. W. T. Hsu, Z. A. Zhao, L. J. Li, C. H. Chen, M. H. Chiu, P. S. Chang, Y. C. Chou, and W. H. Chang, "Second harmonic generation from artificially stacked transition metal dichalcogenide twisted bilayers," ACS Nano **8**, 2951–2958 (2014).
29. K. P. Wang, J. Wang, J. T. Fan, M. Lotya, A. O'Neill, D. Fox, Y. Y. Feng, X. Y. Zhang, B. X. Jiang, Q. Z. Zhao, H. Z. Zhang, J. N. Coleman, L. Zhang, and W. Josef, "Ultrafast saturable absorption of two-dimensional MoS_2 nanosheets," ACS Nano **7**, 9260–9267 (2013).
30. S. X. Wang, H. H. Yu, H. J. Zhang, A. Z. Wang, M. W. Zhao, Y. X. Chen, L. M. Mei, and J. Y. Wang, "Broadband few-layer MoS_2 saturable absorbers," Adv. Mater. **26**, 3538–3544 (2014).
31. J. Du, Q. K. Wang, G. B. Jiang, C. W. Xu, C. J. Zhao, Y. J. Xiang, Y. Chen, S. C. Wen, and H. Zhang, "Ytterbium-doped fiber laser passively mode locked by few-layer molybdenum disulfide (MoS_2) saturable absorber functioned with evanescent field," Sci. Rep. **4**, 6346 (2014).
32. H. Zhang, S. B. Lu, J. Zheng, J. Du, S. C. Wen, D. Y. Tang, and K. P. Loh, "Molybdenum disulfide (MoS_2) as a broadband saturable absorber for ultra-fast photonics," Opt. Express **22**, 7249–7260 (2014).
33. H. D. Xia, H. P. Li, C. Y. Lan, C. Li, X. X. Zhang, S. J. Zhang, and Y. Liu, "Ultrafast erbium-doped fiber laser mode-locked by a CVD-grown molybdenum disulfide (MoS_2) saturable absorber," Opt. Express **22**, 17341–17348 (2014).
34. H. Liu, A. P. Luo, F. Z. Wang, R. Tang, M. Liu, Z. C. Luo, W. C. Xu, C. J. Zhao, and H. Zhang, "Femtosecond pulse erbium-doped fiber laser by a few-layer MoS_2 saturable absorber," Opt. Lett. **39**, 4591–4594 (2014).
35. B. Xu, Y. J. Cheng, Y. Wang, Y. Z. Huang, J. Peng, Z. Q. Luo, H. Y. Xu, Z. P. Cai, J. Weng, and R. Moncorgé, "Passively Q-switched $Nd:YAlO_3$ nanosecond laser using MoS_2 as saturable absorber," Opt. Express **22**, 28934–28940 (2014).
36. Z. Q. Luo, Y. Z. Huang, M. Zhong, Y. Y. Li, J. Y. Wu, B. Xu, H. Y. Xu, Z. P. Cai, J. Peng, and J. Weng, "1-, 1.5-, and 2-μm fiber lasers Q-switched by a broadband few-layer MoS_2 saturable absorber," J. Lightwave Technol. **32**, 4077–4084 (2014).
37. S. Bertolazzi, J. Brivio, and A. Kis, "Stretching and breaking of ultrathin MoS_2," ACS Nano **5**, 9703–9709 (2011).
38. B. Radisavljevic, A. Radenovic, J. Brivio, V. Giacometti, and A. Kis, "Single-layer MoS_2 transistors," Nat. Nanotechnol. **6**, 147–150 (2011).
39. H. Li, Q. Zhang, C. C. R. Yap, B. K. Tay, T. H. Edwin, A. Olivier, and D. Baillargeat, "From bulk to monolayer MoS_2: evolution of Raman scattering," Adv. Funct. Mater. **22**, 1385–1390 (2012).
40. T. Li and G. Galli, "Electronic properties of MoS_2 nanoparticles," J. Phys. Chem. C **111**, 16192–16196 (2007).
41. Z. C. Luo, M. Liu, H. Liu, X. W. Zheng, A. P. Luo, C. J. Zhao, H. Zhang, S. C. Wen, and W. C. Xu, "2 GHz passively harmonic mode-locked fiber laser by a microfiber-based topological insulator saturable absorber," Opt. Lett. **38**, 5212–5215 (2013).
42. F. Lou, Z. T. Jia, J. L. He, R. W. Zhao, J. Hou, Z. W. Wang, S. D. Liu, B. T. Zhang, and C. M. Dong, "Efficient high-peak power wavelength-switchable femtosecond Yb:LGGG laser," IEEE Photon. Technol. Lett. **27**, 407–410 (2015).
43. S. Sahoo, A. P. S. Gaur, M. Ahmadi, M. J.-F. Guinel, and R. S. Katiyar, "Temperature-dependent Raman studies and thermal conductivity of few-layer MoS_2," J. Phys. Chem. C **117**, 9042–9047 (2013).
44. W. Li, J. Carrete, and N. Mingo, "Thermal conductivity and phonon linewidths of monolayer MoS_2 from first principles," Appl. Phys. Lett. **103**, 253103 (2013).